Journal of Radiation and Nuclear Applications
An International Journal

http://dx.doi.org/10.18576/jrna/040203

Modifications of Structural, Optical, and Carbonaceous Clusters in Neutron Irradiated $C_{12}H_{18}O_7$ Polymeric Detector

Y. S. Rammah[1*], *A. R. El-Sersy*[2], *I. A. El-Mesady*[1] *and F.I. El-Agawany*[1]

[1]Department of Physics, Faculty of Science, Menoufia University, 32511 Shebin El-Koom, Egypt.
[2]Department of Ionizing Radiation, National Institute for Standards, El-Haram, P.O. 136, Giza 12211, Egypt.

Received: 23 Mar. 2019, Revised: 1 Apr. 2019, Accepted: 22 Apr. 2019.
Published online: 1 May 2019.

Abstract: The chemical, optical, and carbonaceous clusters properties of CR-39 detectors irradiated at high neutron doses were investigated. They were exposed to neutron source for different times to obtain varies doses. Fourier Transform Infrared (FTIR) and UV-vis spectroscopy have been done for pristine and CR-39 irradiated samples. The chemical and optical properties changes of CR-39 corresponding to the neutron exposure were obtained. In FTIR spectra, the intensities of the absorbance peaks showed a decrease with increasing neutron doses. The UV-vis spectra of the pristine and irradiated CR-39 detectors were analyzed to discuss the induced changes after irradiation. The optical energy band gap, $E_{optical}$ for samples was calculated using Tauc's and absorption spectrum fitting (ASF) methods. Urbach's energy, E_{Urbach} for the samples was estimated. Carbonaceous clusters including number of carbon atom per conjugated length (N) and number of carbon atom per clusters (M) corresponding to the optical band gap, $E_{optical}$ were calculated. In addition, refractive index (n) for pristine and neutron irradiated samples was calculated. Values of optical band gaps displayed a significant decreasing trend in both of direct and indirect transitions, whereas values of N, M, and n increased with neutron dose. Results reveal that CR-39 can be used as neutron dosimetry.

Keywords: CR-39; Neutron irradiation; FTIR; UV-vis; Optical band gap; Dosimetry.

1 Introduction

In general, polymeric materials are affected by radiation exposure with different respondent degrees. These effects are dependent on the radiation parameters and target properties. The resultant induced changes in materials are always due to direct and indirect ionization processes. Fast neutrons interact with polymeric materials via elastic and inelastic nuclear reactions. In case of polymeric track materials, the induced changes are mainly produced from recoiling protons and other fragmentations which are lead to the formation of latent tracks. Tracks in polymers are also associated with the formation of active free radical species which lead to changes in the material morphology, physical and chemical properties. Such changes in material structure might leads to possible uses of the material in different dosimetrical applications.

CR-39 ($C_{12}H_{18}O_7$) is one of the polymeric solid state nuclear track detectors (PSSNTDs) widely used in field of charged particles and neutron spectroscopy produced from both accelerator and reactor facilities as well as different dosimetric studies [1-13]. The importance of CR-39 detector has rapidly increased; it has low price, low weight, surfaces of high quality, and easy manufacturing in thin and thick species [14]. CR-39 is characterized by a chemical composition which is close to that of human's soft tissues which makes it frequently applicable in charged particles and neutron dosimetry [15]. Radiation interacts with polymers such as CR-39 to produce; chain scission, chain aggregation, formation of double bonds and molecular emission. As a consequence, the optical, electrical, mechanical, chemical and track properties of the polymer can be modified [16-24]. Several investigations have been introduced for deep insight into the optical properties of the polymers exposed to different types of radiation such as electrons, alpha particles and swift heavy ions [25-34].

The objective of this study is to investigate the changes in structural and optical characterizations of CR-39 polymeric detectors that induced by fast neutron irradiation by

*Corresponding author e-mail: dr_yasser1974@yahoo.com

recording UV-vis and FTIR spectra for irradiated and non-irradiated samples. These neutron-induced effects are then correlated to the resulted – parameter changes to study the capability of using CR-39 in field of neutron dosimetry. The relative change in the peak intensity associated to the functional groups existent in the polymers have been used to evaluate the relative change in the bond. The optical energy band gap, $E_{optical}$ for irradiated samples was calculated using Tauc's and absorption spectrum fitting (ASF) methods. Urbach's energy, E_{Urbach} for the samples was estimated. Carbonaceous clusters including number of carbon atom per conjugated length (N) and number of carbon atom per cluster (M) that corresponding to the optical energy band gap, $E_{optical}$ was calculated. In addition, refractive index (n) for pristine and neutron- irradiated samples was calculated.

2 Experimental Procedures

In the present study, a poly allyl diglycol carbonate (PADC), a form of CR-39 (TASTRACK) plastic nuclear track detector with molecular formula of ($C_{12}H_{18}O_7$) with1000 μm thickness, and density 1.29 g/cm^3 was used. A large sheet of CR-39 detector is cut carefully into pieces with dimensions of 1x1 cm^2 by laser beam. Four samples were exposed to Am-Be neutron source with activity of 5 mCi and manufactured by Amersham Co., UK, and located at the National Institute of Standards (NIS) of Egypt. The average energy of the Am–Be neutron source is 4.5 MeV according to the technical report of the source [35]. The four samples were irradiated in contact for different duration time, i.e, 2h, 4h, 6h, and 18h to attain various desirable doses. UV-Visible spectra were measured for the irradiated samples to analyze the optical and chemical changes induced at different neutron doses using (Jasco V-576 (Japan) model double-beam spectrophotometer. They were recorded in the spectral range of 190-1100 nm. The FTIR spectrum was recorded in in the range of 400-4000 cm^{-1} using perkinelmer 8000 FTIR spectrophotometer.

3 Theoretical Considerations

3.1 Optical Energy Band Gap, $E_{optical}$

The useful method to evaluate the optical properties for amorphous and crystalline materials like; the optical energy band gap, $E_{optical}$ and refractive index, n is through the studying of the absorption spectra in the UV region for the materials. As a result of interaction between the electrons in the valence bands and electromagnetic waves, some of them are raised to the conduction band. The optical transitions can be occurred by two different ways; direct and indirect transition and both are forbidden or allowed. In this study, the optical energy band gap for the studied samples were evaluated using Tauc's [36] and absorption spectrum fitting (ASF) methods [37, 38].

3.1.1. Tauc's Method, $E_{optical}^{Tauc}$

The optical absorption coefficient (α) was determined at different wavelengths using the relation [39]:

$$\alpha(h\nu) = 2.303\frac{A(h\nu)}{d} \quad (1)$$

Where *A (hν)* is the absorbance, it is given by $A = \log (I_o/I)$, where I_o and I are the intensity of incident and transmitted beams, respectively. *d* is the sample thickness in cm. The absorption coefficient of non-crystalline materials is defined as a function of optical energy gap between the valance and the conduction bands, $E_{optical}$ and the photons energy *hν* by Tauc's [36] and modified by Davis and Mott through the following relation [40]:

$$[\alpha(\nu)h\nu]^{1/m} = K\left(h\nu - E_{optical}\right) \quad (2)$$

where *hν* is the incident photon energy and $E_{optical}$ is the optical energy gap value. *m* has values 0.5, 1.5, 2 and 3 for direct allowed, direct forbidden, indirect allowed and indirect forbidden transitions, respectively [36]. K is assumed to be constant within the frequency range and depends on the probability of the transition. By plotting $(\alpha h\nu)^{1/m}$ against (*hν*) the value of $E_{optical}^{Tauc}$ can be determined. In which, $(\alpha h\nu)^2$ *and* $(\alpha h\nu)^{1/2}$ *against* the photon energy (*hν*) are used to obtain the direct and indirect band gaps, respectively by extrapolating the straight part of the curve.

3.1.2. Absorption Spectrum Fitting (ASF) Method, $E_{optical}^{ASF}$

The optical band gap can be obtained independent on the samples thickness from the film absorbance spectra data [37, 38]. By applying the Beer–Lambert's law in Eq. (1), Eq. (2) can be rewritten as the following [37, 38]:

$$\alpha(\lambda) = K(hc)^{m-1}\lambda\left(\frac{1}{\lambda} - \frac{1}{\lambda_{optical}}\right)^m \quad (3)$$

where $\alpha(\lambda)$ is absorption coefficient. $\lambda_{optical}$, *c,* and *h* are the cut-off wavelength corresponding to the optical gap, velocity of the light, and Planck's constant, respectively. Equation (3) can be simplified to be:

$$A(\lambda) = D\lambda\left(\frac{1}{\lambda} - \frac{1}{\lambda_{optical}}\right)^m \quad (4)$$

where $D = [K(hc)^{m-1} d/2.303]$. The energy band gap determined directly from $\lambda_{optical}$ by the following relation:

$$E_{optical}^{ASF} = \frac{hc}{\lambda_{optical}} = \frac{1239.83}{\lambda_{optical}} \quad (5)$$

From extrapolating the linear region of $(A/\lambda)^{1/m}$ against to (λ^{-1}) curve at $(A/\lambda)^{1/m} = 0$, value of $\lambda_{optical}$ can be deduced.

3.2 Urbach's Energy, E_{Urbach}

A first region in the absorption edge which can be observed in the UV-VIS region where the absorption coefficient, $\alpha < 10^4$ cm^{-1} known as Urbach tail. Urbach energy, E_{Urbach} is the width of band tail energy of the localized-states and given by the following equation [41]:

$$\alpha = \alpha_o \exp\left(\frac{E}{E_{Urbach}}\right) \quad (6)$$

where α_o is a constant, $E=h\nu$ is the photon energy.

3.3 Refractive Index, n

The refractive indices, n are evaluated from optical energy band gap for the studied samples using the following relation [42, 43]:

$$\left(\frac{n^2-1}{n^2+2}\right) = 1 - \left(\frac{E_{optical}}{20}\right)^{1/2} \quad (7)$$

3.4 Carbonaceous Cluster N and M

For a linear structure the number of carbon atoms per conjugation length, N, is given by [44]:

$$N = \frac{2\beta\pi}{E_{optical}} \quad (8)$$

Where the value of β is taken to be -2.9 eV as it is associated with π–π* optical transitions in –C=C– structure and 2β gives the band structure energy of a pair of adjacent π sites. In addition, the number of carbon atoms per cluster, *M*, is given by [44]:

$$M = \left(\frac{34.3}{E_{optical}}\right)^2 \quad (9)$$

4 Results and Discussion

4.1 FTIR Spectroscopy

FTIR spectra between normalized absorbance (%) versus wavenumber (cm^{-1}) in the Attenuated Total Reflection (ATR) mode for unirradiated and neutron-irradiated CR-39 polycarbonate detector films are shown in Fig.1 in the wavenumber range of 400-4000 cm^{-1}. The characteristics of the absorption bands and peak positions for pristine and high neutron irradiated samples are shown in Table 1. The obtained data depicts that, except for the peak at 2927 cm^{-1}, which corresponds to CH_2 group asymmetric stretching, a decrease was observed in the peak intensities with increasing the neutron dose. This decrease may be attributed to the production of more recoil tracks resulted in participation of a large number of chains in the deformation at higher doses. However, no significant shift was observed in the peak positions after neutron irradiation. The maximum change in transmittance value was recorded at positions 1261 and 1745 cm^{-1}. Assignments of FTIR bands of CR-39 polymer films quoted by other authors are listed in Table 1. In addition, effect of neutron irradiation on CR-39 polymeric samples produced an absorption peak at 3441 cm^{-1} corresponds to O-H stretching, H-bonded group (strong and board peak). Another absorption peak grows at 1533 cm^{-1} corresponds to C=C stretching with medium and weak intensity.

The change in the absorbance value with neutron-exposure time was studied in the present work. Three absorption peaks at wave numbers 1745, 1261, and 788 cm^{-1} were chosen as most intense ones (see Fig.1), which expected to have high sensitivity to neutron radiation. The dependences of these absorption peaks on irradiation time are depicted in Fig.2. Fig.2 shows linearity dependences that represented at three values of wave numbers, but their slopes are different, which indicates that different degrees of deformation were obtained for different functional groups. In addition, one can notice that the decrease in absorbance of the peak at 1261 cm^{-1} due to C-O-C aliphatic ester asymmetric stretching, was more significant (highest slope) than these in the absorbance of the other two peaks at 1745 cm^{-1} due to ester C=O group stretching and of the peak at 788 cm^{-1} due to =C-H fragment bending. This implies that the effect on the symmetric stretching of the C-O-C aliphatic ester group produced by neutron exposure is the strongest compared with other groups.

4.2 UV-Visible Spectroscopy

The UV-vis spectra of pristine and neutron irradiated CR-39 polymeric detector is shown in Fig.3. The absorption edge is shifted towards longer wavelength with increasing irradiation time (increase of neutron doses) which may be caused by neutron exposure - induced defects in the polymers. This indicates a decrease in band gap energy of irradiated samples as a result of some electronic levels created inside the forbidden gap. This leads to an increase in the electrical conductivity of the neutron irradiated samples [30,44]. This behavior may be due to the formation of extended system of conjugated bonds, in which, conjugated C=C bonds produced from cleavage of C-C bond and dehydrogenation of the polymer chains resulted from neutron irradiation. Increase in the numbers of conjugated C=C bonds, shifted the absorption band towards higher wavelength with the increase in neutron doses [45]. The absorption bands in the investigated range of wavelength are associated to the π-π* electronic transitions [44]. This type of transitions occurs in the unsaturated centers of the molecules i.e. in compounds containing double or triple bonds and also in aromatics. The excitation of π electron requires smaller energy and hence, transition of this type occurs at longer wavelengths.

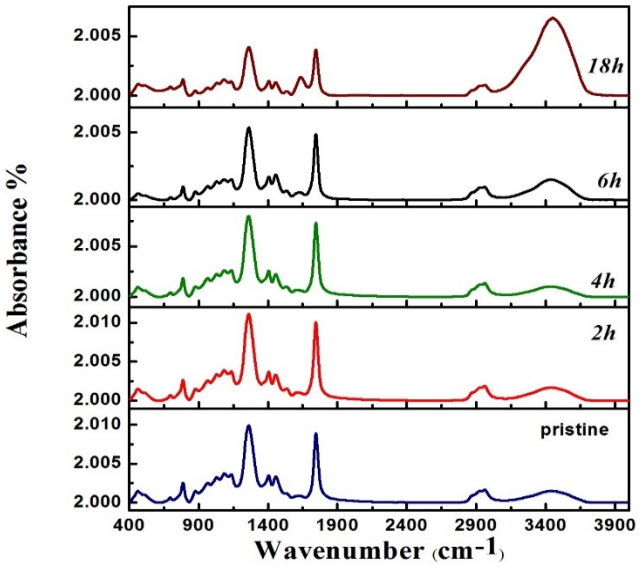

Fig.1: FTIR spectra of normalized absorbance versus wavenumber for pristine and neutron irradiated CR-39 samples.

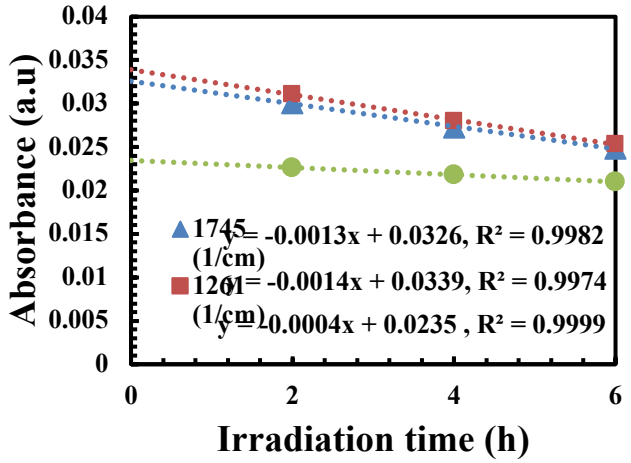

Fig.2: Dependences of the FTIR absorbances at various wave numbers on the neutron irradiation time.

4.2.1 Determination of Optical Energy Band Gap, $E_{optical}$

4.2.1.1 Tauc's method, $E_{optical}^{Tauc}$

The values of optical energy band gap for the pristine and neutron irradiated CR-39 polymeric samples were obtained using Eq.(2). The best fit of indirect allowed transitions is obtained for $m = 2$, meanwhile for a direct allowed transition the best fit is obtained for $m = 1/2$. The indirect and direct band gap was determined respectively from the plot of $(\alpha h\nu)^{1/2}$ and $(\alpha h\nu)^{2}$ versus the photon energy $(h\nu)$. The point at which the first derivative of the plot was maximal, means the linear portion of the plot beyond the inflection point was extrapolated to the $(h\nu)$ axis yields the indirect and direct band gap for pristine and irradiated samples. Figs. 4 and 5. depict the dependencies of $(\alpha h\nu)^{1/2}$ and $(\alpha h\nu)^{2}$ on $(h\nu)$, respectively, from which the optical band gaps for indirect and direct transitions were obtained for pristine and neutron irradiated polymeric samples. The values of different transition energies, $E_{optical}^{Tauc}$ are collected in Table 2. The obtained values reveal the simultaneous existence of indirect and direct band gap in CR-39 polymer detector with decreasing tendency at higher neutron dose. This decreasing may be attributed to the recoil ions produced in the neutron- irradiated CR-39 samples which caused bond breaking and chain scission. This might have resulted in the formation of an allowed state in the forbidden band or in a deformation of the valence band (V.B) [14]. However, the band gap for indirect transitions was found to be narrower than the corresponding band gap for direct transitions.

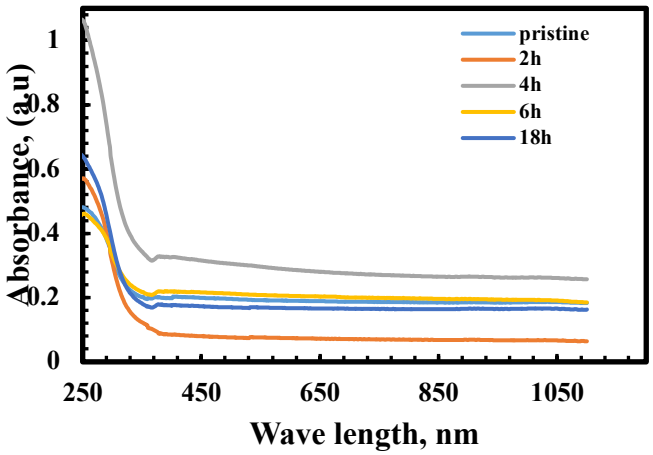

Fig.3: UV-vis spectra of the pristine and neutron irradiated CR-39 samples.

4.2.1.2 Absorption Spectrum Fitting (ASF) Method, $E_{optical}^{ASF}$

The optical band gap can be calculated by the absorption spectrum fitting (ASF) method without any need to the film thickness using Eq.(4) and the parameter $\lambda_{optical}$ in Eq.(5). The dependence of $(A/\lambda)^{0.5}$ and $(A/\lambda)^{2}$ on $(1/\lambda)$ were illustrated in Figs. 6 and 7, respectively. Values of $E_{optical}^{ASF}$ are summarized in Table 3. Results of ASF band gap values for the samples under study were found to be in good agreement with that reported by Tauc's model. Whereas, values of energy gaps of indirect and direct band gaps in CR-39 polymer detectors decrease with increasing neutron doses. Furthermore, the values of band gap for indirect transition have been found to be narrower than the corresponding band gap direct transition.

Table 1: Characteristics of the prominent peaks in the FTIR spectra of the pristine and irradiated CR-39 samples.

Absorption band cm^{-1}	Pristine Peak position cm^{-1}	18h irradiation peak position cm^{-1}	Functional group	Peak absorbance Pristine	Peak absorbance 18h
710-801	788	787	= C - H bending	0.022555	0.021346
802-898	879	877	= C - H bending	0.0215	0.02042
900-980	967	966	C=C-H out of plane deformation	0.022549	0.02066
982-1054	1031	1033	C-O-C aliphatic ester stretching	0.02325	0.021072
1057-1105	1087	1084	C-O-C ether asymmetric stretching	0.023718	0.021347
1105-1162	1136	1136	C-O-C aliphatic ester symmetric stretching	0.023605	0.021184
1163-1321	1261	1261	C-O-C aliphatic ester asymmetric stretching	0.029908	0.024073
1340-1420	1405	1406	symmetric deformation CH_3	0.023487	0.021224
1425-1500	1456	1455	CH_3 , CH_2 deformation	0.023351	0.021108
1650-1790	1745	1745	Ester C=O stretching	0.028859	0.023858
2823-3015	2927	2928	CH_2 asymmetric stretching	0.021505	0.020838

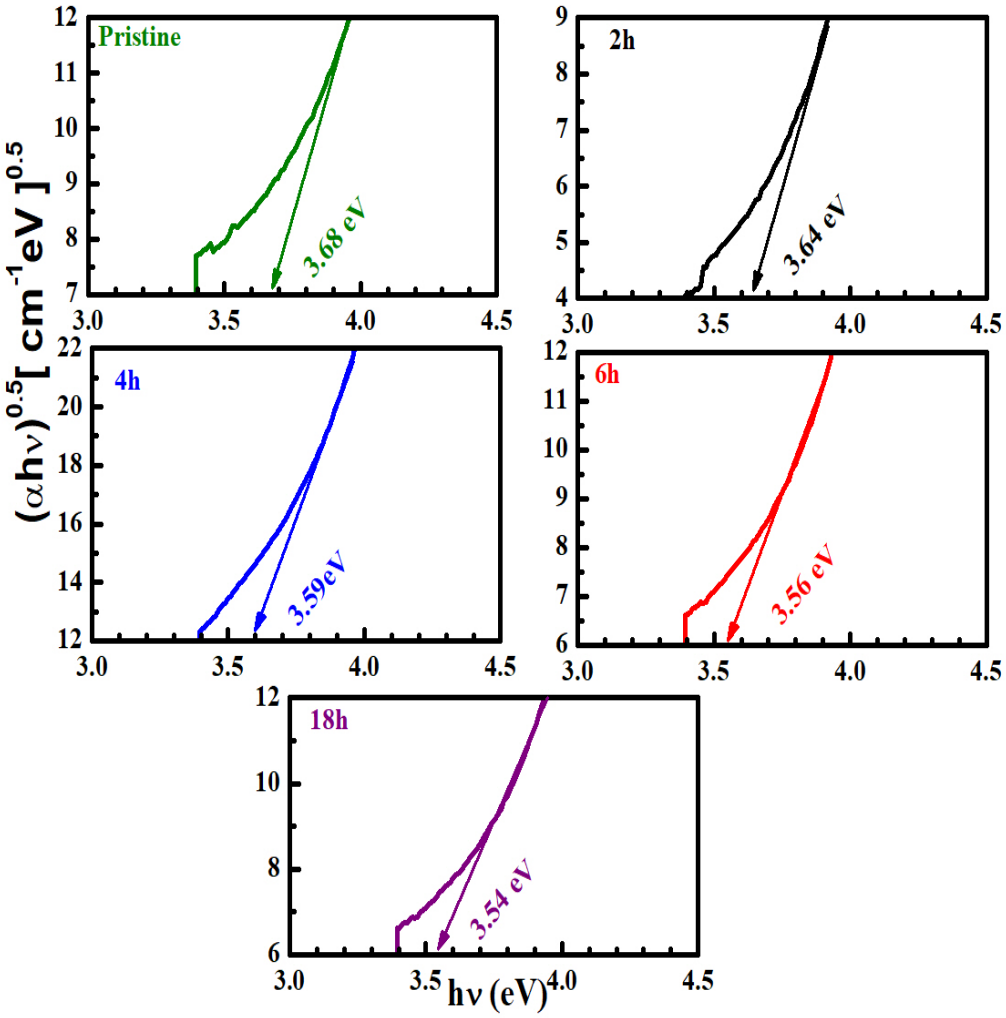

Fig.4: Dependences of $(\alpha h\nu)^{0.5}$ on hν for pristine and neutron irradiated CR-39 samples in Tauc's model.

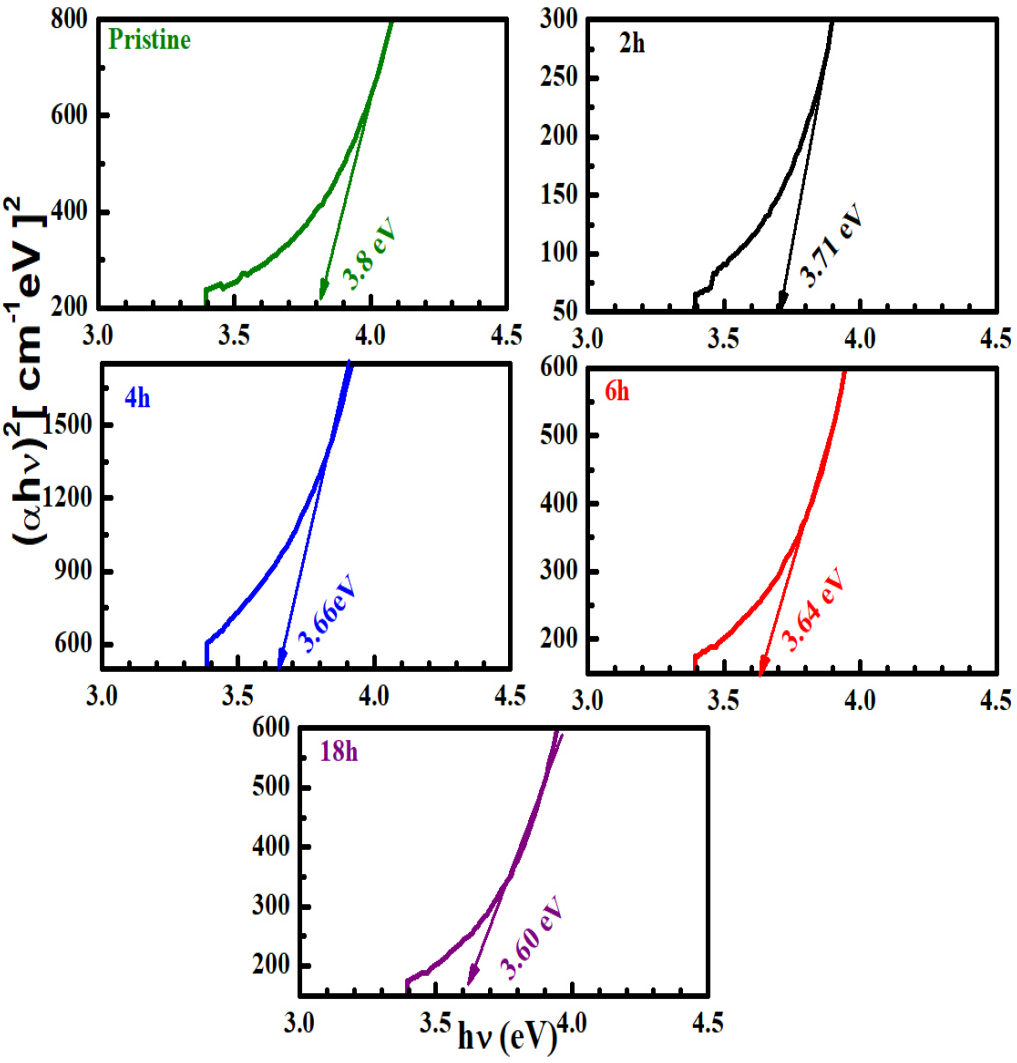

Fig.5: Dependences of $(\alpha h\nu)^2$ on hν for pristine and neutron irradiated CR-39 samples in Tauc's model.

Table 2: Optical band gap, $E_{optical}^{Tauc}$, Urbach's energy, E_{Urbach}, number of carbon atom per conjugated length (N), number of carbon atom per clusters (M), and refractive index (n) for pristine and neutron irradiated CR-39 samples obtained from Tauc's method.

Irradiation time (h)	*Optical band gap, $E_{optical}^{Tauc}$ (eV)*		*Urbach's energy, E_{Urbach} (eV)*	*Number of carbon atom per conjugated length (N)*		*Number of carbon atom per clusters (M)*		*Refractive index (n)*	
	Indirect	Direct		Indirect	Direct	Indirect	Direct	Indirect	Direct
0	3.68	3.8	0.96	4.95	4.79	~ 87	~ 81	2.23	2.21
2	3.64	3.71	0.50	5.0	4.91	~ 89	~ 85	2.24	2.23
4	3.59	3.66	0.76	5.07	4.98	~ 91	~ 88	2.25	2.24
6	3.56	3.64	1.04	5.12	5.0	~ 93	~ 89	2.26	2.24
18	3.54	3.6	0.62	5.14	5.06	~ 94	~ 91	2.27	2.25

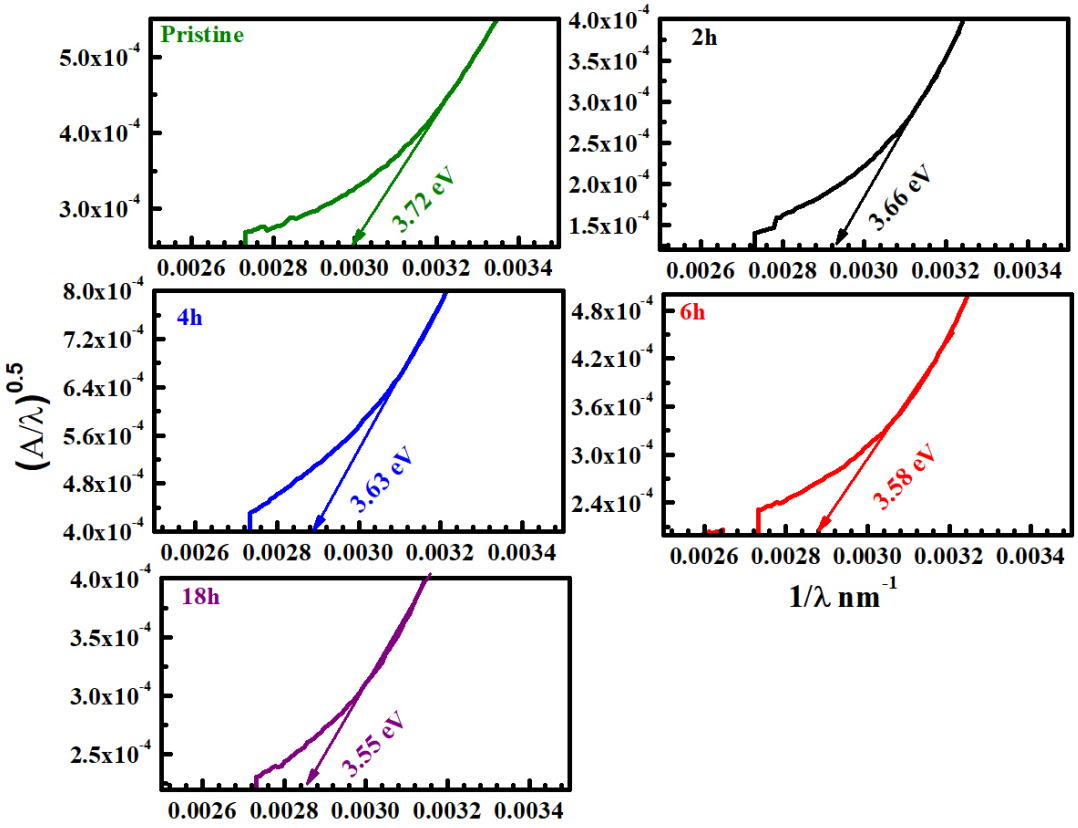

Fig.6: Dependences of $(A/\lambda)^{0.5}$ on λ^{-1} for pristine and neutron irradiated CR-39 samples in ASF method.

Table 3: Optical band gap, $E_{optical}^{ASF}$, number of carbon atom per conjugated length (N), number of carbon atom per clusters (M), and refractive index (n) for pristine and neutron irradiated CR-39 samples obtained from ASF method.

Irradiation time (h)	*Optical band gap, $E_{optical}^{ASF}$ (eV)*		*Number of carbon atom per conjugated length (N)*		*Number of carbon atom per clusters (M)*		*Refractive index (n)*	
	Indirect	Direct	Indirect	Direct	Indirect	Direct	Indirect	Direct
0	3.72	3.88	4.90	4.69	~ 85	~ 78	2.23	2.19
2	3.66	3.77	4.98	4.83	~ 88	~ 83	2.24	2.22
4	3.63	3.72	5.01	4.90	~ 89	~ 85	2.24	2.23
6	3.58	3.68	5.08	4.95	~ 92	~ 87	2.26	2.23
18	3.55	3.61	5.14	5.05	~ 94	~ 90	2.26	2.25

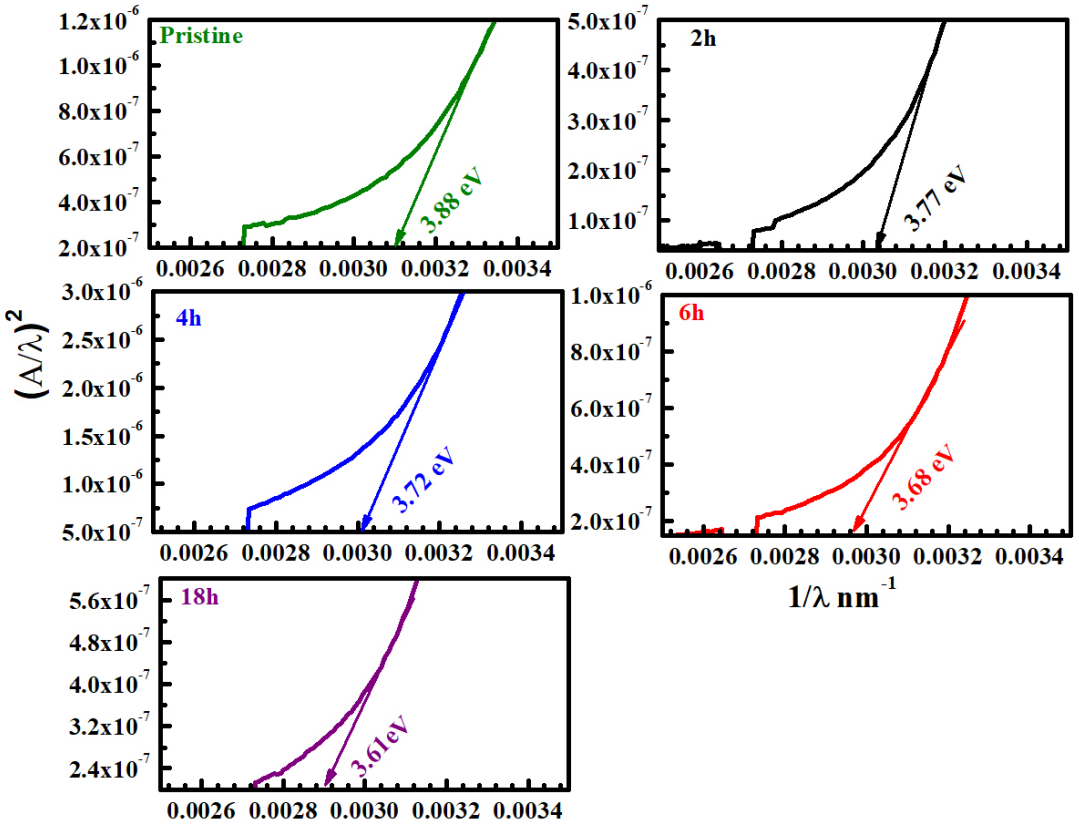

Fig.7: Dependences of $(A/\lambda)^2$ on λ^{-1} for pristine and neutron irradiated CR-39 samples in ASF method.

4.2.2 Urbach's Energy, E_{Urbach}

The importance of Urbach's tail is reflected in understanding the electronic transport phenomenon in the materials. The electronic density of states of amorphous materials is different than that of the crystalline with broadened peaks and decays into the optical energy band gap. In addition, the density of states leads to strains in the network and able to push states past the band edges into the gap. The energy associated with such diffusion is termed as Urbach's energy and used to study the disordering processes in solids. Using Eq. (6), variation in the logarithm of the absorption coefficient (lnα) with the photon energy (hν) for all un-irradiated and neutron irradiated samples was investigated. Inverse of the slope of the linear portion of the curves was used to estimate the Urbach's energies, E_{Urbach} [41]. Values E_{Urbach} are listed in Table 2, in which, a considerable variation was observed in Urbach's energy values with increasing irradiation doses resulting in disorganization in the CR-39 structure [14].

4.2.3 Refractive Index, n

The refractive index, n of CR-39 samples can be calculated as a function of the energy gap for direct and indirect transitions using relation (7). Values of refractive index for the pristine and samples irradiated by neutron are summarized in Tables 2 and 3. The obtained values reveal that the refractive index of the present samples for indirect transitions are slightly higher than those for direct transitions, and the n-value increases slowly with increasing of neutron dose. This result indicates that neutron irradiated CR-39 polymeric detectors is promising in many applications such as optoelectronic devices, in which, the refractive index distribution strongly effects on the wave propagation.

4.2.4 Carbonaceous Cluster N and M

In organic polymers along the swift heavy ions or neutrons trajectory, carbon atoms from the polymer chains are releasing forming which are known as carbon clusters. The absorption edge in the UV-vis spectra is more helpful to get information about this process [45, 46]. Using values of optical band gap energies, $E_{optical}$, the number of carbon atoms per conjugate length, N and the number of carbon atoms per cluster, M were estimated (see Eq; 8 and 9). The obtained values of N and M in Tauc's model are reported in Table 2 and that in ASF model are summarized in Table 3. It is clear that N and M show an increase with doses of neutrons for both indirect and direct transitions, which confirms formation of extended systems of conjugate bonds

as a result of irradiation. However, N and M values for the indirect transitions are higher than those for the direct transitions in the two models.

5 Conclusions

The changes in structural and optical characterization induced by neutron irradiation of CR-39 polymeric detectors and the capability of using these changes on CR-39 to be a good neutron dosimeter have been investigated. FTIR and UV-Vis spectroscopy were performed on pristine and neutron irradiated CR-39 polymeric detectors. Results of analyzed FTIR and UV-vis spectra reveal the following observations: Pristine and neutron irradiated CR-39 detectors characterized by prominent absorbance peaks at 1745, 1261, and 788 cm^{-1} due to ester C=O group stretching, C-O-C aliphatic ester asymmetric stretching, and =C-H fragment bending, respectively. The intensities of most absorbance peaks reduce significantly with neutron irradiation dose. Unknown neutron dose can be estimated from the linear relationship between the peak absorbance and neutron dose. The optical energy band gap for both indirect and direct transitions decrease with increasing neutron dose, it takes values in the range of 3.68-3.54 eV, and 3.8-3.6 eV for indirect and direct transitions, respectively in Tauc's model, while takes values 3.72-3.55 and 3.88-3.61 for indirect and direct transition, respectively in ASF model,urbach's energy varies with neutron irradiation dose. Number of carbon atoms per conjugate length, N and per cluster, M were increased with neutron irradiation dose and CR-39 polymeric detector can be used as neutron dosimeter.

Acknowledgements: The author gratefully acknowledges and wishes to express their appreciation to Prof. Dr. A. Hussein, Physics Department, Faculty of Science, Menoufia University, Egypt for his fruitful help, valuable comments, and his helping to achievement this work.

References

[1] A. Abdalla, et al., Fast neutrons detection in CR-39 and DAM–ADC nuclear track detectors, Radiation Physics and Chemistry., **108**, 24-28, 2015.

[2] D. Al-Azmi, et al., Indoor radon in Kuwait, Health physics., **94 (1)**, 49-56, 2008.

[3] M. Al-Jarallah, et al., Correlation between radon exhalation and radium content in granite samples used as construction material in Saudi Arabia, Radiation Measurements., **40(2-6)**, 625-629, 2005.

[4] E. Awad, et al., Alpha spectroscopy in CR-39 SSNTDs using energy simulation and matrix of energy equations for open field studies, Physics Letters A., **372(17)**, 2959-2966, 2008.

[5] E. Awad, et al., Alpha particle spectroscopy for CR-39 detector utilizing matrix of energy equations, Physics Letters A., **369(5-6)**, 359-366, 2007.

[6] R. Bedogni and E. Fantuzzi, A personal neutron monitoring system based on CR-39 recoil proton track detectors: assessment of Hp (10) using Image process algorithms, Radiation protection dosimetry., **10 (4-1)** , 183-186, 2002.

[7] I. Csige, et al., Environmental effects on induction time and sensitivity of different types of CR-39, International Journal of Radiation Applications and Instrumentation. Part D. Nuclear Tracks and Radiation Measurements., **19(1-4)** ,151-154, 1991.

[8] F. Erees et al., Measurements of radon content in soil gas and in the thermal waters in Western Turkey, Radiation measurements., **41(3)**, 354-361, 2006.

[9] E. Fantuzzi, et al., Performance of CR-39® with addition of DOP (dioctylphthalate) for fast neutron dosimetry, Radiation measurements., **36(1-6)**, 475-478, 2003.

[10] Z. Tayyeb, et al., A study on the radon concentrations in water in Jeddah (Saudi Arabia) and the associated health effects, Journal of environmental radioactivity., **38(1)**, 97-104, 1998.

[11] L. Tommasino, et al., Cosmic-ray neutron spectrometry by solid state detectors, Radiation measurements., **36(1-6)** ,307-311, 2003.

[12] M. Zaki and Y. El-Shaer, Particularization of alpha contamination using CR-39 track detectors, Pramana., **69(4)** ,567-574, 2007.

[13] D. Zhou et al., Radiation field of cosmic rays measured in low Earth orbit by CR-39 detectors, Advances in Space Research, 37(9) ,1764-1769, 2006.

[14] M. Zaki, Gamma-induced modification on optical band gap of CR-39 SSNTD, Journal of Physics D: Applied Physics., **41(17)** ,175404, 2008.

[15] D. Zhou et al., LET calibration for CR-39 detectors in different oxygen environments, Radiation Measurements., **42 (9)** ,1499-1506, 2007.

[16] R. Kumar et al., Study of optical band gap and carbonaceous clusters in swift heavy ion irradiated polymers with UV–Vis spectroscopy, Nuclear Instruments And Methods In Physics Research Section B: Beam Interactions With Materials And Atoms., **266(8)**, 1788-1792, 2008.

[17] R. Mishra et al., Electron induced modification in poly (ethylene terephthalate), Radiation effects and defects in solids., **153(3)**, 257-269, 2001.

[18] R. Mishra et al., Optical and electrical properties of some electron and proton irradiated polymers, Nuclear Instruments and Methods in Physics Research Section B: Beam Interactions with Materials and Atoms., **168(1)**, 59-64, 2000.

[19] T. Phukan et al., Dielectric response of heavy ion irradiated PADC track detector, Nuclear Instruments and Methods in Physics Research Section B: Beam Interactions with Materials and Atoms., **155(1-2)**, 116-119, 1999.

[20] L. Singh et al., Opto-chemical response of CR-39 and

polystyrene to swift heavy ion irradiation, Nuclear Instruments and Methods in Physics Research Section B: Beam Interactions with Materials and Atoms., **255(2)** , 350-356, 2007.

[21] D. Sinha and K. Dwivedi, Modifications of radiation detection response of PADC track detectors by photons, Radiation Physics and Chemistry., **53(2)** , 99-105, 1998.

[22] D. Sinha et al., Gamma ray photon-induced modifications in Triafol-TN and Triafol-BN polymeric track detectors, Radiation measurements., **29(6)** , 599-604, 1998.

[23] A. Tidjani and Y. Watanabe, Gamma-oxidation of linear low-density polyethylene: The dose–rate effect of irradiation on chemical and physical modifications, Journal of Polymer Science Part A: Polymer Chemistry., **33(9)**, 1455-1460, 1995.

[24] Z. Zhu et al., Chemical modifications of ion irradiated polystyrene probed by optical absorption measurements, Nuclear Instruments and Methods in Physics Research Section B: Beam Interactions with Materials and Atoms., **166**, 621-626, 2000.

[25] C. Chong et al., UV-VIS and FTIR spectral studies of CR-39 plastics irradiated with X-rays, Radiation Measurements., **28(1-6)**, 119-122, 1997.

[26] M. El Hofy and H. Elsamman, Optical density of the etched α-tracks in CR-39 nuclear track detector, Radiation measurements., **29(5)**, 461-464, 1998.

[27] Z. Mokrani et al., Characterization of chemical and optical modifications induced by 22.5 MeV proton beams in CR-39 detectors, Radiation measurements., **36(1-6)**, 615-620., 2003.

[28] T. Phukan et al., Study of optical properties of swift heavy ion irradiated PADC polymer, Radiation measurements., **36(1-6)**, 611-614, 2003.

[29] A. F. Saad et al., Radiation-induced modifications on spectroscopic and thermal properties of CR-39 and SR-90 nuclear track detectors, Radiation measurements., **40(2)**, 780-784, 2005.

[30] S. Singh and S. Prasher, UV–VIS spectroscopic and etching studies of IR exposed CR-39 plastic track detector, Nuclear Instruments and Methods in Physics Research Section B., **215(1)**, 169-173, 2004.

[31] S. Singh and S. Prasher, A comparison of modifications induced by Li3+ and O6+ ion beam to Makrofol-KG and CR-39 polymeric track detectors, Nuclear Instruments and Methods in Physics Research Section B., **244(1)**, 252-256, 2006.

[32] S. Singh and S. Prasher, The etching and structural studies of gamma irradiated induced effects in CR-39 plastic track recorder, Nuclear Instruments and Methods in Physics Research Section B: Beam Interactions with Materials and Atoms., **222(3-4)**, 518-524, 2004.

[33] K. C. C. Tse et al., Photo-degradation of PADC by UV radiation at various wavelengths, Polymer Degradation and Stability., **91(10)** , 2380-2388, 2006.

[34] T. Yamauchi et al., Track core size estimation for heavy ions in CR-39 by AFM and UV methods, Nuclear Instruments and Methods in Physics Research Section B., **236(1)**, 318-322, 2005.

[35] Amersham, The Radiochemical Center Technical Bulletin ., **76/7**, 1976.

[36] J. Tauc, Amorphous and liquid semiconductors Springer Science & Business Media, 1974.

[37] D. Souri and K. Shomalian, Band gap determination by absorption spectrum fitting method (ASF) and structural properties of different compositions of (60− x) V2O5–40TeO2–xSb2O3 glasses, Journal of Non-Crystalline Solids., **355(31-33)**, 1597-1601, 2009.

[38] D. Souri and Z. Tahan, A new method for the determination of optical band gap and the nature of optical transitions in semiconductors, Applied Physics B., **119(2)**, 273-279, 2015.

[39] M. Fox, Optical properties of solids AAPT, 2002.

[40] N. F. Mott and E. A. Davies, Electronic Processes in Non-Crystalline Materials, Clarendon Press, Oxford, 1979.

[41] F. Urbach, The long-wavelength edge of photographic sensitivity and of the electronic absorption of solids, Physical Review., **92(5)**, 1324, 1953.

[42] A. Ali et al., FTIR and UV spectra of pentaternary borate glasses, Measurement., **105**, 72-77, 2017.

[43] V. Dimitrov and S. Sakka, Electronic oxide polarizability and optical basicity of simple oxides, Journal of Applied Physics., **79(3)**, 1736-1740, 1996.

[44] D. Nikezic and K. Yu, Formation and growth of tracks in nuclear track materials, Materials Science and Engineering: R: Reports., **46(3-5)**, 51-123, 2004.

[45] B. A. El-Badry et al., An optical method for fast neutron dosimetry using CR-39 Radiation Effects & Defects in Solids., **163(10)**, 821-825, 2008.

[46] D. Fink et al., Carbonaceous clusters in irradiated polymers as revealed by UV-Vis spectrometry, Radiation effects and defects in solids., **133(3)**, 193-208, 1995.